New BIOTECHNOLOGY 41 (2018) 1–8

Contents lists available at ScienceDirect

New BIOTECHNOLOGY

journal homepage: www.elsevier.com/locate/nbt

Full length Article

Biosynthesis of selenium-nanoparticles and -nanorods as a product of selenite bioconversion by the aerobic bacterium *Rhodococcus aetherivorans* BCP1

Alessandro Presentato[a,*], Elena Piacenza[a], Max Anikovskiy[b], Martina Cappelletti[c], Davide Zannoni[c], Raymond J. Turner[a,*]

[a] Microbial Biochemistry Laboratory, Department of Biological Sciences, University of Calgary, 2500 University Dr. NW, Calgary, AB T2N 1N4, Canada
[b] Department of Chemistry, University of Calgary, 2500 University Dr. NW, Calgary, AB T2N 1N4, Canada
[c] Laboratory of General and Applied Microbiology, Department of Pharmacy and Biotechnology, Via Irnerio 42, Bologna, 40126, Italy

ARTICLE INFO

Keywords:
Selenite
Rhodococcus aetherivorans
Selenium nanoparticles
Selenium nanorods
Biogenic nanostructures

ABSTRACT

The wide anthropogenic use of selenium compounds represents the major source of selenium pollution worldwide, causing environmental issues and health concerns. Microbe-based strategies for metal removal/recovery have received increasing interest thanks to the association of the microbial ability to detoxify toxic metal/metalloid polluted environments with the production of nanomaterials. This study investigates the tolerance and the bioconversion of selenite (SeO_3^{2-}) by the aerobically grown *Actinomycete Rhodococcus aetherivorans* BCP1 in association with its ability to produce selenium nanoparticles and nanorods (SeNPs and SeNRs). The BCP1 strain showed high tolerance towards SeO_3^{2-} with a Minimal Inhibitory Concentration (MIC) of 500 mM. The bioconversion of SeO_3^{2-} was evaluated considering two different physiological states of the BCP1 strain, i.e. *unconditioned* and/or *conditioned* cells, which correspond to cells exposed for the first time or after re-inoculation in fresh medium to either 0.5 or 2 mM of Na_2SeO_3, respectively. SeO_3^{2-} bioconversion was higher for *conditioned* grown cells compared to the *unconditioned* ones. Selenium nanostructures appeared polydisperse and not aggregated, as detected by electron microscopy, being embedded in an organic coating likely responsible for their stability, as suggested by the physical-chemical characterization. The production of smaller and/or larger SeNPs was influenced by the initial concentration of provided precursor, which resulted in the growth of longer and/or shorter SeNRs, respectively. The strong ability to tolerate high SeO_3^{2-} concentrations coupled with SeNP and SeNR biosynthesis highlights promising new applications of *Rhodococcus aetherivorans* BCP1 as cell factory to produce stable Se-nanostructures, whose suitability might be exploited for biotechnology purposes.

Introduction

Selenium (Se) is present in the earth crust as a rare element or associated in minerals (e.g., crooksite and calusthalite), with concentrations ranging from 0.01 to 1200 mg/kg [1–3]. It is an essential micronutrient for living systems, being present as seleno-cysteine in at least 25 human selenoproteins [4]. Importantly, the physical-chemical properties of Se (e.g., relatively low melting point, high photo- and semi-conductivity, optical responses and catalytic activity) enable its use in several areas of application, namely the electronics and glass industries, animal feeds and food supplements, metal alloys for batteries, production of pigments and plastics [5,6]. However, the anthropogenic misuse of Se-containing compounds has led to an increase of Se content in the environment, primarily in four inorganic forms: selenate (SeO_4^{2-}) and selenite (SeO_3^{2-}) oxyanions, selenide (Se^{2-}), and elemental selenium (Se^0) [6]. Among these, Se^{2-} present in organic compounds (e.g. dimethyl selenide, trimethyl selenonium, selenomethionine, selenocysteine and Se-methylselenocysteine) and Se^0 showed lower toxicity levels [7–9] compared to SeO_4^{2-} and SeO_3^{2-}, which were described as the most toxic, soluble and, consequently, bioavailable forms. Nevertheless, Gram-positive bacteria belonging to the *Bacillus* genus have been noted for their ability to grow in the presence of either SeO_4^{2-} or SeO_3^{2-}, including *Bacillus mycoides* SelTE01, *Bacillus cereus* CM100B and *Bacillus selenitireducens* MLS10 [6,10,11]. Furthermore, *Pantoea agglomerans* UC-32, *Stenotrophomonas maltophilia* SelTE02 and *Shewanella oneidensis* MR-1 have been

* Corresponding authors.
E-mail addresses: alessandro.presentat@ucalgary.ca (A. Presentato), elena.piacenza@ucalgary.ca (E. Piacenza), m.anikovskiy@ucalgary.ca (M. Anikovskiy), martina.cappelletti2@unibo.it (M. Cappelletti), davide.zannoni@unibo.it (D. Zannoni), turnerr@ucalgary.ca (R.J. Turner).

https://doi.org/10.1016/j.nbt.2017.11.002
Received 19 May 2017; Received in revised form 13 November 2017; Accepted 20 November 2017
Available online 21 November 2017
1871-6784/

characterized as some of the Gram-negative SeO_4^{2-}/SeO_3^{2-} bioconverting bacteria [12–14].

It is now recognized that the microbial bioconversion of SeO_3^{2-} into Se^0 leads to the formation of metalloid precipitates and/or nanostructures in the form of nanoparticles (NPs) or nanorods (NRs) [15–17], with features of adsorptive ability, antioxidant functions and remarkable biological reactivity (e.g., anti-hydroxyl radical efficacy and protective effect against DNA oxidation) [17,18]. Se-nanostructures can also exert high antimicrobial activity against human pathogenic bacteria and anticancer activity [19–21]. Up to now, Se-nanostructures have been synthesized mostly by physical or chemical methods through the use of harsh chemicals under extreme system conditions (high temperature and pressure), resulting in high costs of production, the formation of hazardous waste, and consequently the emergence of safety concerns [22]. In contrast, the advantage of using SeO_4^{2-}/SeO_3^{2-} bioconverting bacteria to produce Se-nanomaterials would lead to the development of safe, inexpensive and eco-friendly approaches compared to synthetic procedures [23]. In this context, among the bacterial strains suitable as cell factories for nanotechnology purposes, those belonging to the *Rhodococcus* genus have been described for their environmental robustness and persistence [24], resisting harsh conditions of growth [25,26].

Our previous study reported the ability of *Rhodococcus aetherivorans* BCP1 to resist high concentrations of tellurium in the form of K_2TeO_3 and to produce Te-nanorods (TeNRs) [27]. Thus, based on our prior findings and considering that selenium and tellurium are both metalloid elements sharing common physical-chemical properties, here we demonstrate the potential of the BCP1 strain also to bioprocess high concentrations of SeO_3^{2-} producing Se-nanostructures. In contrast with BCP1 TeO_3^{2-}-grown cells, those grown in the presence of SeO_3^{2-} showed a remarkable proficiency to synthesize simultaneously zero-dimensional (0D) and one-dimensional (1D) Se-nanomaterials (i.e. SeNPs and NRs) upon SeO_3^{2-} bioconversion. This work further demonstrates the suitability of this strain as a cell factory to process and produce diverse nanostructures differently depending on the oxyanion precursor supplied.

Materials and methods

Tolerance of the BCP1 strain towards SeO_3^{2-} and bacterial culture conditions

BCP1 tolerance towards SeO_3^{2-} was evaluated by challenging the bacterial cells for 24 h with increasing concentrations of oxyanion (0–600 mM), while the growth cultures of *unconditioned* and/or *conditioned* BCP1 cells were performed as described in our previous work [27], supplying either 0.5 mM or 2 mM of Na_2SeO_3 to the Luria-Bertani (LB) rich medium. Survival and growth rate of the BCP1 strain were evaluated by the spot plate count method. The number of cells is reported as average of the Colony Forming Unit (log_{10}[CFU/mL]) for each biological trial (n = 3) with standard deviation (SD). All the reagents were purchased from Sigma-Aldrich®.

SeO_3^{2-} bioconversion assay

The residual concentration of SeO_3^{2-} over the incubation time of BCP1 cells has been evaluated as published elsewhere [16]. Briefly, the reaction mixture was prepared by adding 10 mL of 0.1 M HCl, 0.5 mL of 0.1 M EDTA, 0.5 mL of 0.1 M NaF, and 0.5 mL of 0.1 M disodium oxalate in a 25- to 30 mL glass tube. A 50- to 250 µL of culture broth containing 100 to 200 nmol of SeO_3^{2-} was added to the above-described mixture, along with 2.5 mL of 0.1% 2,3-diaminonaphthalene in 0.1 M HCl. After all the reagents were mixed, the mixture was incubated at 40 °C for 40 min and then cooled to room temperature (RT). The selenium-2,3-diaminonaphthalene complex was extracted in 6 mL of cyclohexane by shaking the reaction mixture for 1 min. The absorbance of the organic phase was read at 377 nm using a 1 cm path length quartz cuvette (Hellma®) and a Varian Cary® 50 Bio UV–vis Spectrophotometer. A calibration curve was performed using 0, 50, 100, 150, and 200 nmol of SeO_3^{2-} in LB (R^2 = 0.99). The data are reported as average values (n = 3) with SD. All the manipulations were performed in the dark and the reagents were purchased from Sigma-Aldrich®.

Preparation, recovery and characterization of Se-nanostructure extracts

The extracts containing Se-nanostructures produced by the BCP1 strain were prepared and recovered following the procedure published in our previous study [27]. The characterization of Se-nanostructure extracts was carried out by Transmission Electron Microscopy (TEM), Energy-Dispersive X-ray Spectroscopy (EDX) analysis, Dynamic Light Scattering (DLS) and Zeta potential measurements. A Hitachi H7650 TEM was used to image either Se-nanostructure extracts or BCP1 cells negatively stained using a 1% phosphotungstic acid solution (pH 7.3) air dried onto carbon-coated copper grids (CF300-CU, Electron Microscopy Sciences). The elemental composition of Se-nanostructure extracts was performed using a Zeiss Sigma VP and Oxford Instruments INCAx-act through single point selection analysis of either SeNPs or SeNRs mounted onto Crystalline Silicon wafers (type N/Phos, size 100 mm, University WAFER) carried by Specimen Aluminum stubs (TED PELLA, INC.). DLS and Zeta potential analyses of the samples containing biogenic Se-nanomaterials were measured using Zen 3600 Zetasizer Nano ZS™ from Malvern Instruments as described elsewhere [27].

Results

Tolerance of Rhodococcus aetherivorans BCP1 towards SeO_3^{2-}

The capacity of the BCP1 strain to tolerate increased concentrations of SeO_3^{2-} was established by exposing the cells for 24 h to different Na_2SeO_3 concentrations, ranging from 0 to 600 mM. The data summarized in Fig. 1 showed the high tolerance of the BCP1 strain towards SeO_3^{2-}, with 500 mM as its Minimal Inhibitory Concentration (MIC^{Se}). Indeed, a significant decrease (2 log_{10} reduction) in the number of viable cells counted as compared to their initial amount (1.3×10^6 CFU/mL) was only observed as a result of BCP1 incubation in the presence of high SeO_3^{2-} concentrations, starting from 200 mM (6.2×10^4 CFU/mL).

Bioconversion of SeO_3^{2-} by BCP1 and detection of Se-nanostructures

Two physiological states of the BCP1 strain, here indicated as *unconditioned* and/or *conditioned* cells, were studied to evaluate whether differences occurred in their growth rate and bioconversion extent of either 0.5 or 2 mM of SeO_3^{2-} (Fig. 2), as previously reported for TeO_3^{2-}-grown cells [27]. *Unconditioned* BCP1 cells grown in the presence of 0.5 mM SeO_3^{2-} bioconverted ca. 10% of the initial oxyanion amount during the early stage of the bacterial growth (12 h), while the maximum extent of SeO_3^{2-} bioconversion (62% of its initial concentration) occurred at 120 h of incubation. At this time, a certain level of cell death was also evidenced, the number of viable cells being lower (1.2×10^6 CFU/mL) compared to those not exposed to SeO_3^{2-} (6.8×10^6 CFU/mL) (Fig. 2a). In contrast, 0.5 mM SeO_3^{2-} was completely bioconverted by *conditioned* BCP1 cells within 96 h of incubation, which corresponded to the late exponential growth phase (Fig. 2b).

The growth trend of *unconditioned* cells incubated with 2 mM SeO_3^{2-} (Fig. 2c) resembled that displayed by 0.5 mM SeO_3^{2-}-grown cells (Fig. 2a). Nevertheless, the extent of SeO_3^{2-} removal was ca. 50% of its initial amount (2 mM), occurring slowly and linearly over the timeframe considered (120 h) (Fig. 2c). Furthermore, the resulting yield

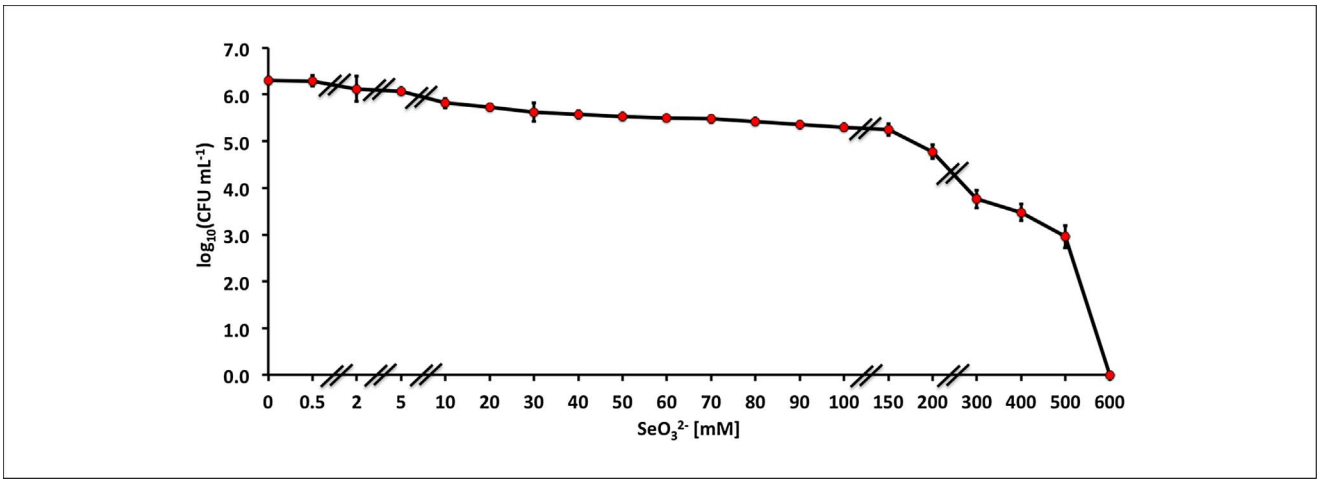

Fig. 1. Tolerance of *Rhodococcus aetherivorans* BCP1 exposed for 24 h to increasing concentrations of Na_2SeO_3. The Minimal Inhibitory Concentration of SeO_3^{2-} (MIC^{Se}) was 500 mM.

of SeO_3^{2-} bioconversion was higher (ca. 74%) under BCP1 *conditioned* growth mode in the presence of 2 mM SeO_3^{2-} (Fig. 2d). Finally, Se-nanostructures in the form of SeNPs and NRs were generated by BCP1 as products of SeO_3^{2-} bioconversion, being mainly located on the outer surface of the cells (Fig. 3).

Transmission electron microscopy (TEM) analysis and size distribution of Se-nanostructure extracts

TEM observations were carried out on Se-nanostructure extracts to study the size and morphology of the nanomaterials isolated from both *unconditioned* and *conditioned* BCP1 cells (Fig. 4). For each growth mode and concentration of Na_2SeO_3 tested (0.5 and 2 mM), BCP1 cells simultaneously synthesized both SeNPs and NRs (indicated as $SeNPs_{0.5}$, $SeNPs_2$, $SeNRs_{0.5}$ and $SeNRs_2$ by arrows in Fig. 4a, b, c and d). These nanostructures were not aggregated, suggesting their natural thermodynamic stability, and surrounded by an electron-dense material. The actual diameter and length of SeNPs and SeNRs, respectively, showed broad distributions, indicating their polydispersity in suspension. SeNPs recovered from *unconditioned* BCP1 cells were characterized by an average size of 71 ± 24 nm ($SeNPs_{0.5}$) and 78 ± 42 nm ($SeNPs_2$), while those isolated from *conditioned* cells showed average sizes of 53 ± 20 nm ($SeNPs_{0.5}$) and 97 ± 21 nm ($SeNPs_2$) (Fig. 5). $SeNRs_{0.5}$ and $SeNRs_2$ displayed average lengths centered at 555 ± 308 nm and 494 ± 261 nm, respectively, while those extracted from *conditioned* cells displayed lengths of 474 ± 279 nm ($SeNRs_{0.5}$) and 444 ± 253 nm ($SeNRs_2$) (Fig. 6).

Energy-dispersive X-Ray spectroscopy (EDX) analyses of Se-nanostructure extracts

The elemental composition analysis of Se-nanomaterial extracts was

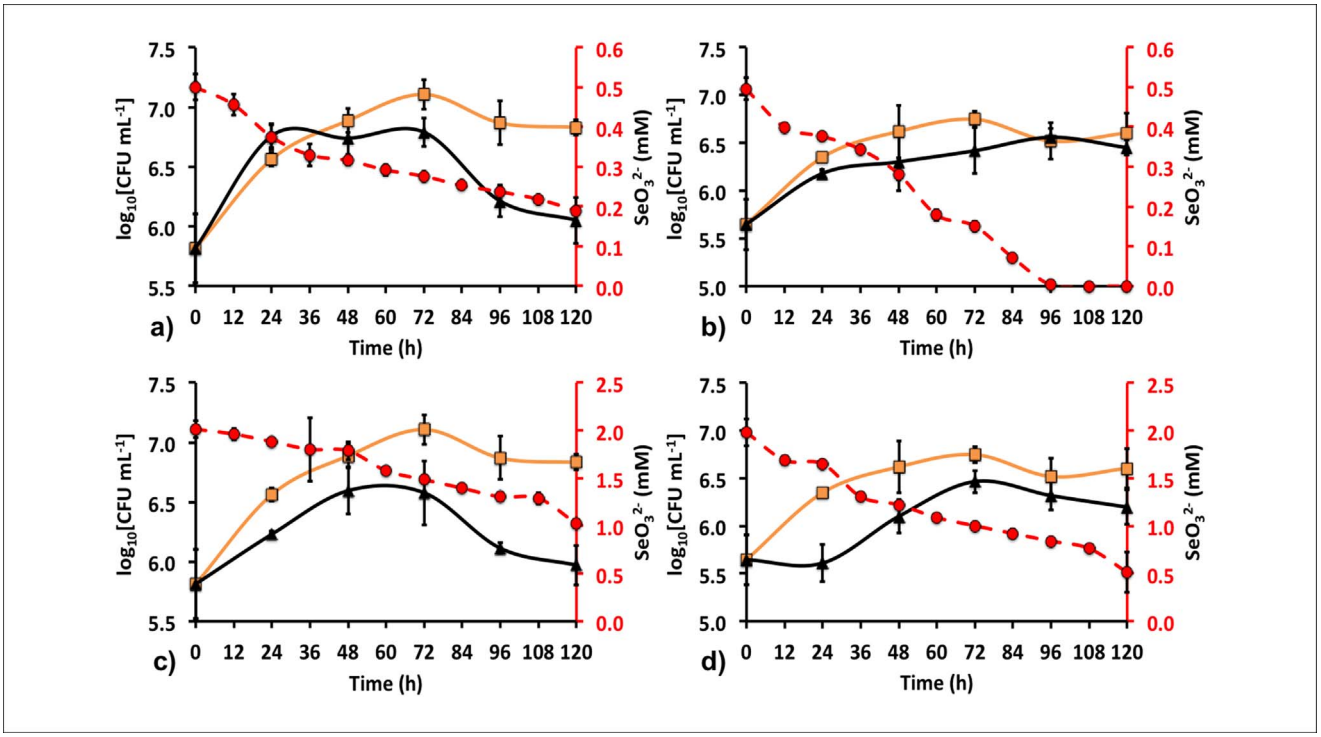

Fig. 2. *Rhodococcus aetherivorans* BCP1 growth in LB medium (orange curves), LB supplied with 0.5 or 2 mM of Na_2SeO_3 (black curves) as *unconditioned* (a and c) or *conditioned* (b and d) cells, and SeO_3^{2-} bioconversion indicated by ashed red curves. (For interpretation of the references to colour in this figure legend, the reader is referred to the web version of this article.)

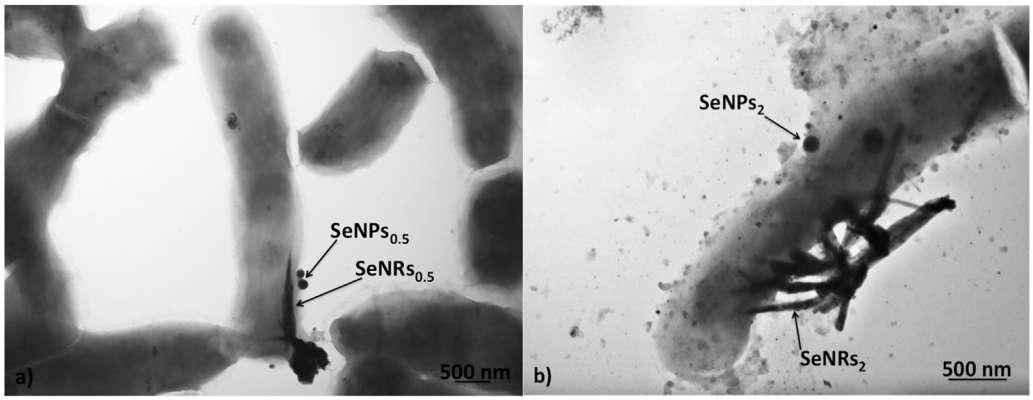

Fig. 3. Transmission Electron Microscopy (TEM) micrographs of BCP1 cells grown for 120 h in the presence of 0.5 mM (a), and 2 mM (b) of Na_2SeO_3. Arrows indicate selenium nanostructures (SeNPs and/or SeNRs) produced by the BCP1 strain.

performed by EDX Spectroscopy (Fig. S1, Table S1 and S2). The presence of silicon in the EDX spectra was due to the silicon stubs onto which the samples were mounted. Excluding the silicon signal, SeNPs and NRs elemental composition showed the presence of the same chemical elements independently of both the growth conditions and the different initial concentrations of the precursor (Na_2SeO_3), being carbon, nitrogen, oxygen and selenium (Fig. S1), for which the relative percentage values are listed in Tables S1 and S2. Only in the case of $SeNPs_2$ and $SeNRs_2$ produced by *conditioned* BCP1 cells were peaks corresponding to carbon and selenium detected (Fig. S1 d and h). The detection of the above elements in addition to selenium in the nanomaterial context suggested the presence of an organic coating surrounding these biogenically produced nanostructures.

Dynamic light scattering (DLS) analysis

Since EDX spectra revealed chemical elements other than Se in the biogenic nanomaterial extracts, it is reasonable to hypothesize that Se-nanostructures may be surrounded by an organic material. In this regard, DLS experiments were carried out on the organic material recovered from the Se-nanostructure samples by centrifugation at 16,000 × *g* for 10 m, to evaluate its capability to self-assemble in the nanoscale range (Fig. S**2**). As a result, all the recovered organic materials showed similar size distributions, being 149 ± 13 nm (0.5 mM)

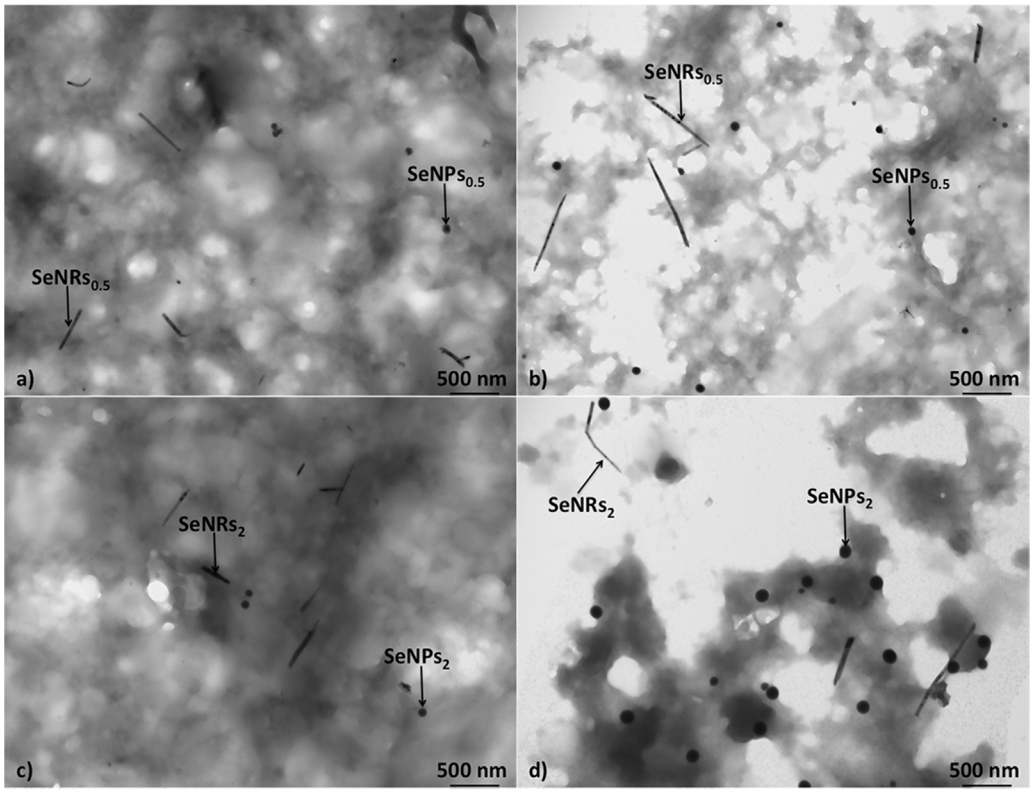

Fig. 4. Transmission Electron Microscopy (TEM) micrographs of *unconditioned* and/or *conditioned* generated $SeNPs/SeNRs_{0.5}$ (a and b) and $SeNPs/SeNRs_2$ (c and d).

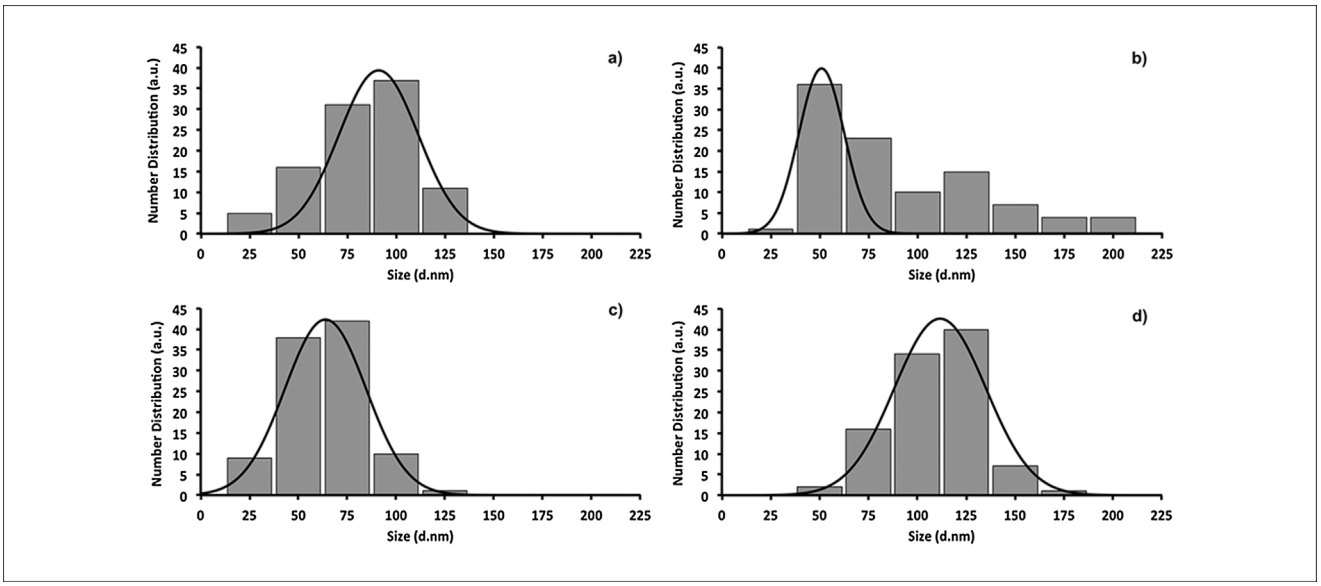

Fig. 5. Size distributions (nm) of $SeNPs_{0.5}$ (a), and $SeNPs_2$ (b) generated by *unconditioned* BCP1 Na_2SeO_3-grown cells, and $SeNPs_{0.5}$ (c), and $SeNPs_2$ (d) isolated from the *conditioned* cells. Size distributions are indicated as histograms, while the Gaussian fit is highlighted as a continuous black curve.

and 157 ± 13 nm (2 mM) for those deriving from Se-nanostructures produced by *unconditioned* cells, or 143 ± 21 nm (0.5 mM) and 123 ± 18 nm (2 mM) for those isolated from nanomaterials generated by *conditioned* cells (Fig. S2 a and b).

Zeta potential measurement

Zeta potential measurements were conducted to evaluate the surface potential of Se-nanostructure extracts (Fig. S3). Two different peaks were detected in zeta potential plots for both *unconditioned* Se-nanostructure extracts generated by BCP1 cells grown in the presence of 0.5 mM (−32 and −27 mV) or 2 mM (−31 and −13 mV) SeO_3^{2-} (Fig. S3a and b). Se-nanostructure extracts recovered from *conditioned* BCP1 cells displayed less negative zeta potential values, being −20 mV (0.5 mM) and −26 mV (2 mM) (Fig. S3c and d). Since Se does not have a net charge, zeta potential measurements were also performed on the organic material recovered after removing Se-nanostructures by centrifugation. Indeed, that recovered from the biogenic nanomaterials produced by *unconditioned* cells revealed surface potential values of −19 (0.5 mM) and −13 mV (2 mM) (Fig. S4a and b), while those from the Se-nanostructure extracts generated by *conditioned* cells had surface potentials of −15 (0.5 mM) and −12 mV (2 mM) (Fig. S4c and d), indicating that the surface charges detected for the Se-nanostructure extracts were due to the presence of charged molecules within the isolated organic material.

Discussion

Among Gram-positive bacteria, several species belonging to a few genera (e.g. *Streptomyces*, *Salinicoccus* and *Bacillus*) have previously been investigated for their potential in bioconverting SeO_3^{2-} along with the production of nanosized structures under aerobic growth conditions [28–30]. Indeed, SeNP production has been widely investigated with anaerobic microorganisms such as *Sulfurospirillum*

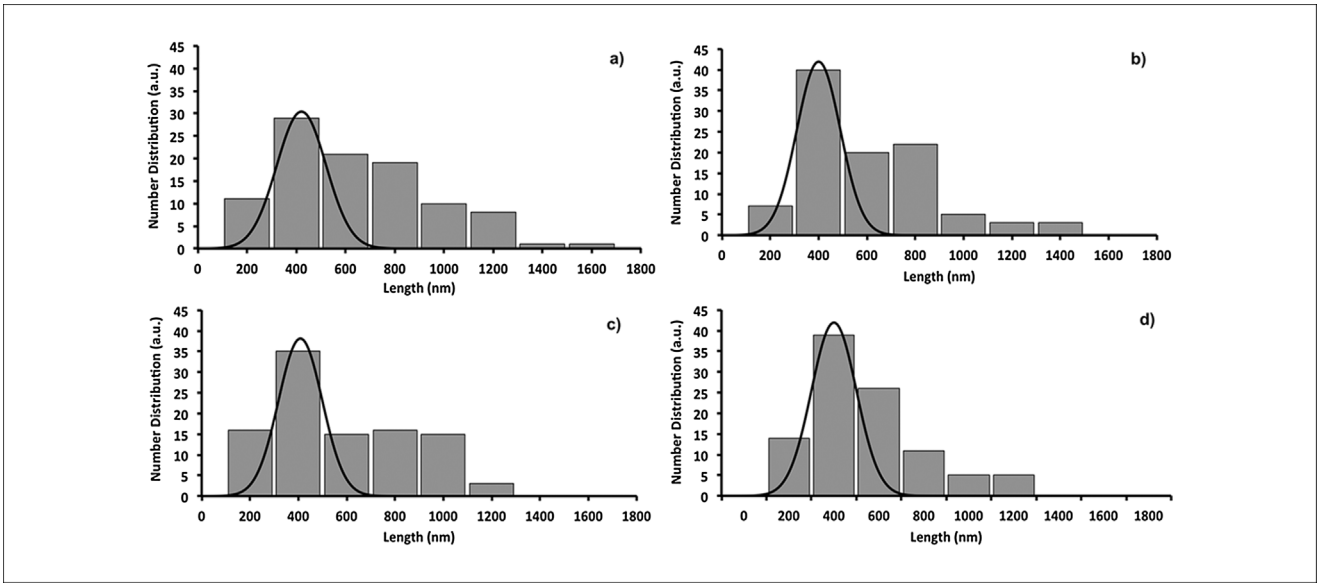

Fig. 6. Length distribution (nm) of $SeNRs_{0.5}$ (a), and $SeNRs_2$ (b) generated by *unconditioned* BCP1 Na_2SeO_3-grown cells, and $SeNRs_{0.5}$ (c), and $SeNRs_2$ (d) isolated from *conditioned* cells Length distributions are indicated as histograms, while the Gaussian fit is highlighted as a continuous black curve.

barnesii, *Bacillus selenitireducens*, *Selenihalanerobacter shriftii*, *Rhodospirillum rubrum*, *Geobacter sulfurreducens*, *Shewanella oneidensis* and *Veillonella atypica*, [11,16,31], among others. However, the exploitation of strictly aerobic rhodococci to produce biogenic metalloid nanomaterials has not been investigated. Indeed, only *Rhodococcus aetherivorans* BCP1 was previously investigated by our group for the biosynthesis of TeNRs [27].

Here, BCP1 cells grown under aerobic conditions showed an elevated tolerance towards SeO_3^{2-} (MIC^{Se} = 500 mM) (Fig. 1) compared to that for TeO_3^{2-} (MIC^{Te} = 11.2 mM) [27], the toxicity exerted by Te-oxyanions on bacterial cells being 100-fold higher than for other metals and metalloids of environmental and public health concern [32]. Moreover, BCP1 exceeded the level of SeO_3^{2-} tolerance observed for the majority of strictly aerobic Gram-positive bacteria described in literature, being one of the bacterial strains with the highest MIC^{Se} value along with *Salinicoccus* sp. QW6 [29] and *Bacillus* sp. STG-83 [30].

The considered timeframe to evaluate the bacterial growth and the concentrations of SeO_3^{2-} tested were chosen on the basis of the following considerations: (i) there was no significant difference between the number of viable cells counted after 24 h exposure to 0.5 mM (2.0×10^6 CFU/mL) or 2 mM (1.7×10^6 CFU/mL) of SeO_3^{2-}; (ii) *Actinomycetes* are known to be slow growing strains (120 h has been used by authors studying SeNPs produced by *Streptomyces microflavus* strain FSHJ31 [28]); (iii) 2 mM SeO_3^{2-} (223 mg kg^{-1}) is a much higher concentration than those found in well-known highly polluted sites worldwide [33–35]. Overall, *conditioned* BCP1 cells showed a higher proficiency towards SeO_3^{2-} bioconversion compared to the *unconditioned* cells (Fig. 2), indicating a greater performance of pre-adapted biomass in the removal of these oxyanions, as also observed in the case of TeO_3^{2-}-grown cells [27].

Research to date suggests that the primary redox buffering molecules glutathione (GSH) and bacillithiol (BSH) are commonly present in *Proteobacteria* and *Firmicutes* respectively, while *Actinobacteria* are mainly characterized by mycothiol (MSH) [36]. In this regard, the established higher redox stability of MSH compared to GSH [37] may explain the capacity of BCP1 cells to grow aerobically and tolerate high concentrations of SeO_3^{2-} under oxidative stress conditions, as described for *Streptomyces* sp. ES2-5 [38]. Moreover, since oxygen is the preferential electron acceptor under oxic growth conditions, SeO_3^{2-} reduction does not generally support aerobic bacterial growth [38]. Thus, the high level of BCP1 resistance towards SeO_3^{2-}, as well as its incomplete bioconversion within 120 h of incubation, may suggest a detoxification mechanism for this oxyanion [39], in line with our previous study and those focused on *Streptomyces* sp. ES2-5 and *Comamonas testosteroni* S44 [27,38,40].

Both anaerobic and aerobic bacterial strains investigated for the production of Se-nanostructures have been described as generating mostly spherical polydisperse SeNPs, ranging in size between 50 and 500 nm [41]. The synthesis of SeNRs was reported in *Pseudomonas alcaliphila*, *Streptomyces bikiniensis* strain Ess_amA-1, *Bacillus subtilis*, and *Ralstonia eutropha* [17,21,42,43]. It is now established that a variation in the temperature [42], in the incubation time [17,21] or growth mode (i.e. growing or resting cells) [43] can stimulate the production and conversion of SeNPs to SeNRs. Conversely, BCP1 simultaneously synthesized these Se-nanostructures on the outer cellular surface (Fig. 3).

The production of Se-nanostructures by BCP1 cells might be explained by the LaMer mechanism of nanoparticle formation [44]. According to this mechanism, upon SeO_3^{2-} bioconversion into Se^0, the Se-atoms as generated organize themselves into Se-nucleation seeds, turning into NPs through a ripening process [44,45]. Considering that a feature of SeNPs is their high free energy and low stability in suspension, they can spontaneously dissolve and release Se-atoms [17,46], which might precipitate as nanocrystallinites in one direction, forming SeNRs [47]. Moreover, smaller SeNPs are featured by a high solubility [48] that results in their rapid dissolution in suspension, generating long SeNRs. In contrast, larger SeNPs are more stable and less prone to dissolution, resulting in the production of short SeNRs. In line with this, BCP1 produced smaller SeNPs on addition of 0.5 mM SeO_3^{2-} (Fig. 5a and c), which led to the formation of longer SeNRs (Fig. 6a and c) compared to those generated from the incubation of bacterial cells with 2 mM SeO_3^{2-} (Fig. 6b and d).

A common feature of nanomaterials is their high thermodynamic instability, which results in their natural tendency to form large aggregates [49,50]. TEM micrographs and EDX spectra revealed the presence of non-aggregated biogenic SeNPs and SeNRs surrounded by an organic electron-dense material (Fig. 4, Fig. S1, Tables S1 and S2). Considering that the natural stability of Se-nanomaterials produced by microorganisms was earlier ascribed to the presence of an organic polymer layer [51,52], the organic material detected surrounding both SeNPs and NRs is likely to be responsible for their stability. Indeed, DLS analyses and zeta potential measurements reinforced the notion of a coating non-covalently associated with SeNPs and SeNRs and involved in their stabilization, similarly to what has been observed for biogenic TeNRs [27]. Thus, DLS analyses suggested that the recovered organic material can auto-assemble in the nanoscale range, indicating the presence of macromolecules that may sterically contribute to the stability of the biogenic Se-nanomaterials. Furthermore, the negative zeta potential values of both Se-nanostructure extracts and the recovered organic material (Fig. S3 and S4) suggested the existence of an electrostatic repulsion interaction between Se-nanostructures and the organic material. Although the organic polymer layer plays a key role as electrosteric stabilizer of biogenic nanomaterials [52], its composition is yet to be elucidated. In this regard, it is noteworthy to mention that surfactant-like molecules are generally utilized to stabilize chemically synthesized nanomaterials [48]. Since *Rhodococcus* species are described as producers of surfactant-like molecules [53,54], it is reasonable to consider that the electrosteric stabilization of the Se-nanostructures might be mediated by amphiphilic surfactant-like molecules co-produced by BCP1.

Conclusion

The present study demonstrates the high resistance of BCP1 towards SeO_3^{2-} (MIC^{Se} = 500 mM), as well as its proficiency in bioconverting these oxyanions. This bioconversion can be exploited to generate different morphologies of Se-nanostructures (NPs and NRs), unlike TeO_3^{2-}-grown cells that were only able to generate TeNRs [27]. Further, biogenic SeNPs and NRs are stabilized in suspension by the presence of a surrounding organic material, as also observed for TeNRs produced by BCP1 [27]. Finally, the concentration of provided SeO_3^{2-} precursor was crucial in determining both the size and length of SeNPs and SeNRs, respectively. Thus, these findings further support the suitability of the BCP1 strain as a cell factory for chalcogen-based nanomaterial synthesis.

Ethics in publishing

Not applicable.

Declaration of interest

The authors declare that they have no competing interests.

Submission declaration and verification

The authors declare that this work is not published elsewhere and that it is approved for publication.

Author contributions

AP, Post-doctoral fellow in the Microbial Biochemistry Laboratory

at the Department of Biological Sciences of Calgary University, contributed to the scientific development of this study, namely: (i) performing of the experiments, (ii) data interpretation, (iii) major contribution to the writing of the manuscript.

EP, PhD student in the Department of Biological Sciences of Calgary University, was the second major contributor to the writing of the manuscript, fundamental for the Transmission and Scansion Electron Microscopy imaging and data analyses.

MA, instructor at the Chemistry Department of the University of Calgary, participated in the characterization analyses of Se-nanostructures along with the interpretation of the data and editing of the physical-chemical part of the manuscript.

MC, research associate in the Laboratory of General and Applied Microbiology at the Department of Pharmacy and Biotechnology of the University of Bologna, participated in the revision of the manuscript, providing important suggestions for improved interpretation of the biological results.

DZ, full professor and coordinator of the Laboratory of General and Applied Microbiology at the Department of Pharmacy and Biotechnology of the University of Bologna, provided the *Rhodococcus aetherivorans* BCP1 strain and contributed intellectually to the interpretation and development of this study.

RJT, full professor and principal investigator of the Microbial Biochemistry Laboratory at the Department of Biological Sciences of the University of Calgary, made major intellectual and financial contributions during the development of this study, managing and directing the research as well as editing and revising the manuscript.

Funding

This study was funded by Natural Science and Engineering Research Council of Canada (NSERC).

Acknowledgments

The Natural Science and Engineering Research Council of Canada (NSERC) is gratefully acknowledged for support of this study. We also acknowledge the Nanoscience Program at the University of Calgary for providing access to SEM, EDX, DLS, and zeta-potential measurements and the Microscopy Imaging Facility (MIF) at the University of Calgary for providing access to TEM.

Appendix A. Supplementary data

Supplementary data associated with this article can be found, in the online version, at https://doi.org/10.1016/j.nbt.2017.11.002.

References

[1] Ralston NVC, Ralston CR, Blackwell III JL, Raymond LJ. Dietary and tissue selenium in relation to methylmercury toxicity. Neurotoxicology 2008;29:802–11.
[2] Keller EA. Keller EA, editor. Earth Materials and Processes. Environmental Geology. 9th editionUpper Saddle River Prentice Hall; 2010 Chapter 2.
[3] Reilly C. Reilly C, editor. Introduction. Selenium in Food and Health. 2nd editionNew York: Springer Science + Business Media; 2006. p. 1–18 Chapter 1.
[4] Mehdi Y, Hornick J, Istasse L, Dufrasne I. Selenium in the Environment, Metabolism and Involvement in Body Functions. Molecules 2013;18:3292–311.
[5] Craig PJ, Maher W. Craig PJ, editor. Organoselenium compounds in the environment. Organometallic Compounds in the Environment. 2nd editionChichester: Jon Wiley & Sons; 2003. p. 391–8 Chapter 10.
[6] Lampis S, Zonaro E, Bertolini C, Bernardi P, Butler CS, Vallini G. Delayed formation of zero-valent selenium nanoparticles by *Bacillus mycoides* SelTE01 as a consequence of selenite reduction under aerobic conditions. Microb Cell Fact 2014;13:35.
[7] Selenium Barceloux DG. Toxicol Clin Toxicol 1999;37(2):145–72.
[8] Martens DA, Suarez DL. Selenium speciation of soil/sediment determinated with sequential extractions and hydride generation atomic absorption spectrophotometry. Environ Sci Technol 1996;31:133–9.
[9] Kyriakopoulos A, Behne D. Selenium-Containing proteins in mammals and other of life. In: Amara SG, Blaustein MP, Jahn R, Miyajima A, Pfanner N, Scheiger M, editors. Reviews of Physiology Biochemistry and Pharmacology 145. Berlin: Springer-Verlag Berlin Heidelberg; 2002. p. 5 Chapter 1.
[10] Dhanjal S, Cameotra SS. Aerobic biogenesis of selenium nanosphere by *Bacillus cereus* isolated from coal mine soil. Microb Cell Fact 2010;5(9):52.
[11] Oremland RS, Herbel MJ, Blum JS, Langley S, Beveridge TJ, Ajayan PM, et al. Structural and spectral features of selenium nanospheres produced by Se-respiring bacteria. Appl Environ Microbiol 2004;70(1):52–60.
[12] Torres SK, Campos VL, Leon CG, Rodriguez-Llamazares SM, Rojas SM, Gonzalez M, et al. Biosynthesis of selenium nanoparticles by *Pantoea agglomerans* and their antioxidant activity. J Nanopart Res 2012;14:1236–9.
[13] Antonioli P, Lampis S, Chesini I, Vallini G, Rinalducci S, Zolla L, et al. *Stenotrophomonas maltophilia* SelTE 02 a new bacterial strain suitable for bioremediation of Selenite-Contaminated Environmental Matrices. Appl Environ Microbiol 2007:6854–63.
[14] Klonowska A, Heulin T, Vermeglio A. Selenite and Tellurite reduction by *Shewanella oneidensis*. Appl Environ Microbiol 2005;560:7–560. 9.
[15] Silverberg BA, Wong PTS, Chau YK. Localization of selenium in bacterial cells using TEM and energy dispersive X-ray analysis. Arch Microbiol 1976;107:1–6.
[16] Kessi J, Ramuz M, Wehrli E, Spycher M, Bachofen R. Reduction of Selenite and detoxification of elemental selenium by the phototropic bacterium *Rhodospirillum rubrum*. Appl Environ Microbiol 1999;65(11):4734–40.
[17] Zhang W, Chen Z, Liu H, Zhang L, Gao P, Li D. Biosynthesis and structural characteristics of selenium nanoparticles by *Pseudomonas alcaliphila*. Colloid Surf B 2011;88:196–201.
[18] Wang H, Zhang J, Yu H. Elemental selenium at nano size posseses lower toxicity without compromising the fundamental effect on selenoenzymes: comparison with selenomethionine in mice. Free Radic Biol Med 2007;42:1524–33.
[19] Tran PA, Webster TJ. Selenium nanoparticles inhibit *Staphylococcus aureus* growth. Int J Nanomed 2011;6:1553–8.
[20] Piacenza E, Presentato A, Zonaro E, Lemire JA, Demeter M, et al. Antimicrobial activity of biogenically produced spherical Se-nanomaterials embedded in organic material against *Pseudomonas aeruginosa* and *Staphylococcus aureus* strains on hydroxyapatite-coated surfaces. Microbiol Biotechnol 2017;10:804–18. http://dx.doi.org/10.1111/1751-7915.12700.
[21] Ahmad MS, Yasser MM, Sholkamy EN, Ali AM, Mehanni MM. Anticancer activity of biostabilized selenium nanorods synthesized by *Streptomyces bikiniensis* strain Ess_amA-1. Int J Nanomed 2015;10:3389–401.
[22] Ingale AG, Chaudhari AN. Biogenic synthesis of nanoparticles and the potential applications: an EcoFriendly approach. J Nanomed Nanotechnol 2013;4:165.
[23] Wadhwani SA, Shedbalkar U, Singh R, Chopade BA. Biogenic selenium nanoparticles: current status and future prospects. Appl Microbiol Biotechnol 2016;100:2555–66.
[24] Martínková L, Uhnáková B, Pátek M, Nesvera J, Kren V. Biodegradation potential of the genus *Rhodococcus*. Environ Int 2009;35:162–77.
[25] Cappelletti M, Presentato A, Milazzo G, Turner RJ, Fedi S, et al. Growth of *Rhodococcus* sp: strain BCP1 on gaseous n-alkanes: new metabolic insights and transcriptional analysis of two soluble di-iron monooxygenase genes. Front Microbiol 2015;6:393.
[26] Orro A, Cappelletti M, D'Ursi P, Milanesi L, Di Canito A, et al. Genome and phenotype microarray analyses of *Rhodococcus* sp. BC and *Rhodococcus opacus* R7: genetic determinants and metabolic abilities with environmental relevance. PLoS One 2015;10(10):P1.
[27] Presentato A, Piacenza E, Anikovskiy M, Cappelletti M, Zannoni D, Turner RJ. *Rhodococcus aetherivorans* BCP1 as cell factory for the production of intracellular tellurium nanorods under aerobic conditions. Microb Cell Fact 2016;15:204.
[28] Forootanfar H, Zare B, Fasihi-Bam H, Amirpour-Rostami S, Ameri A, Shakibaie M. Biosynthesis and characterization of selenium nanoparticles produced by terrestial actinomycete streptomyces microflavus strain FSHJ31. Research and reviews. J Microbiol Biotechnol 2014;3:47–53.
[29] Amoozegar MA, Ashengroph M, Malekzadeh F, Razavi MR, Naddaf S, Kabiri M. Isolation and initial characterization of the tellurite reducing moderately halophilic bacterium, *Salinicoccus* sp. strain QW6. Microbiol Res 2008;163:456–65.
[30] Soudi MR, Ghazvini PTM, Khajeh K, Gharavi S. Bioprocessing of seleno-oxyanions and tellurite in a novel *Bacillus* sp: strain STG-83: a solution to removal of toxic oxyanions in presence of nitrate. J Hazard Mater 2009;165:71–7.
[31] Pearce CI, Pattrick RAD, Law N, Charnock JM, Coker VS, Fellowes JW, et al. Investigating different mechanisms for biogenic selenite transformations: geobacter sulfuureducens, Shewanella oneidensis and Veillonella atypica. Environ Technol 2009;30:1313–26.
[32] Harrison JJ, Ceri H, Stremick CA, Turner RJ. Biofilm susceptibility to metal toxicity. Environ Microbiol 2004;6:1220–7.
[33] Rogers P, Arora SP, Fleming GA, Crinion R, McLaughlin JG. Selenium toxicity in farm-animals – treatment and prevention. Irish Vet J 1990;43:151–3.
[34] Presser TS, Ohlendorf HM. Biogeochemical cycling of selenium in the San Joaquin Valley, California USA. Environ Manage 1987;11:805–21.
[35] Sharma N, Prakash R, Srivastava A, Sadana US, Acharya R, et al. Profile of selenium in soil and crops in seleniferous area of Punjab, India by neutron activation analysis. J Radioanal Nucl Chem 2009;281:59–62.
[36] Fahey RC. Glutathione analogs in prokaryotes. BBA-Bioenergetics 2013;1830(5):3182–98.
[37] Newton GL, Ta P, Fahey RC. A mycothiol synthase mutant of Mycobacterium smegmatis produces novel thiols and has an altered thiol redox status. J Bacteriol 2005;187:7309–16.
[38] Tan Y, Yao R, Wang R, Wang D, Wang G, Zheng S. Reduction of selenite to Se(0) nanoparticles by filamentous bacterium *Streptomyces* sp: ES2-5 isolated from a selenium mining soil. Microb Cell Fact 2016;15:157.
[39] Lovley DR. Dissimilatory metal reduction. Ann Rev Microbiol 1993;47:263–90.
[40] Zheng S, Su J, Wang L, Yao R, Wang D, et al. Selenite reduction by the obligate

aerobic bacterium *Comamonas testosteroni* S44 isolated from a metal-contaminated soil. BMC Microbiol 2014;14:204–16.
[41] Shirsat S, Kadam A, Naushad M, Mane RS. Selenium nanostructures: microbial synthesis and applications. RSC Adv 2015;5:92799–811.
[42] Wang T, Yang L, Zhang B, Liu J. Extracellular biosynthesis and transformation of selenium nanoparticles and application in H_2O_2 biosensor. Colloid Surf B Biointerfaces 2010;80:94–102.
[43] Srivastava N, Mukhopadhyay M. Green synthesis and structural characterization of selenium nanoparticles and assessment of their antimicrobial property. Bioprocess Biosyst Eng 2015;38:1723–30.
[44] Thanh NTK, Maclean N, Mahiddine S. Mechanisms of nucleation and growth of nanoparticles in solution. Chem Rev 2014;114:7610–30.
[45] Gates B, Mayers B, Cattle B, Xia Y. Synthesis and characterization of uniform nanowires of trigonal selenium. Adv Funct Mater 2002;12:219–27.
[46] Gates B, Yin Y, Xia Y. A solution-phase approach to the synthesis of uniform nanowires of crystalline selenium with lateral dimensions in the range of 10–30 nm. J Am Chem Soc 2000;122:12582–3.
[47] Jeong U, Camargo PHC, Lee YH, Xia Y. Chemical transformation: a powerful route to metal chalcogenide nanowires. J Mater Chem 2006;16:3893–7.
[48] Cao G. Cao G, editor. Physical Chemistry of Solid Surface. In: Cao G, editor. Nanostructures and Nanomaterials, synthesis, properties and applications. London: Imperial College Press; 2004. p. 15–48 Chapter 2.
[49] Goldstein AN, Echer CM, Alivisatos AP. Melting in semiconductor nanocrystals. Science 1991;256:1425.
[50] Roco MC. Nanoparticles and nanotechnology research. J Nanoparticle Res 1999:1–6.
[51] Kessi J, Hanselmann KW. Similarities between the abiotic reduction of selenite with glutathione and the dissimilatory reaction mediated by *Rhodospirillum rubrum* and *Escherichia coli*. J Biol Chem 2004;279:50662–9.
[52] Winkel LHE, Johnson CA, Lenz M, Grundl T, Leupin OX, et al. Environmental selenium research: from microscopic processes to global understanding. Environ Sci Technol 2012;46:571–9.
[53] Rapp P, Bock H, Wray V, Wagner F. Formation, isolation and characterization of trehalose dimycolates from *Rhodococcus erythropolis* grown on n-alkanes. J Gen Microbiol 1979;115:491–503.
[54] Kim JS, Powalla M, Lang S, Wagner F, Lunsdorf H, Wray V. Microbial glycolipid production under nitrogen limitation and resting cell condition. J Bacteriol 1990;13:257–66.